and 128.7 (aromatic CH's), 12.44 and 12.19 ppm (Me's); Mass (EI), m/e 77, 178, 342 (M).

10. Spectral data of **7**; UV (MeOH), λ_{max} 320, 253 nm; ^{1}H NMR ($CDCl_3$), δ 7.98-7.45 (10H), 2.08 (6H, s), 1.39 ppm (6H, s); Mass (EI), m/e 342 (M).
11. Spectral data of **10**; IR (KBr), 3057, 2924, 2185, 1665, 1447, 1376, 758 cm^{-1}; UV (MeOH), λ_{max} 248, 312 nm; ^{1}H NMR ($CDCl_3$), δ 7.89-7.28 (10H), 2.00 (3H), 1.97 (3H), 1.66 (3H), 1.52 ppm (3H); ^{13}C NMR ($CDCl_3$), δ 194.1 and 193.5 (C=O's), 131.9, 128.8, 128.6, 128.4, 128.2 and 126.5 (aromatic CH's), 16.50, 15.41, 13.93 and 13.66 ppm (Me's); Mass (EI), m/e 202, 366 (M).
    Spectral data of **11**; UV (MeOH), λ_{max} 320, 281, 272, 252, 244 nm; ^{1}H NMR ($CDCl_3$), δ 7.80-7.38 (10H), 2.12 (3H, s), 1.67 (3H, s), 1.41 (3H, s), 1.40 ppm (3H, s); Mass (EI), m/e 202, 366 (M).
    Spectral data of **12**; IR (KBr), 3064, 2931, 1658, 1447, 1377, 786, 695 cm^{-1}; UV (MeOH), λ_{max} 259, 270 nm; ^{1}H NMR ($CDCl_3$), δ 7.28-7.04 (2 x 5H), 2.04 (6H, s), 1.89 (6H, s), 1.66 (6H, s), 1.58 ppm (6H, s); ^{13}C NMR ($CDCl_3$), δ 200.2 and 198.0 (C=O's), 128.7, 128.0 and 126.1 (aromatic CH's), 16.28, 16.10, 13.21 and 13.53 (Me's), 150.7, 141.9, 141.8, 138.7, 132.2, 59.24 and 56.75 ppm (7 C's); Mass (EI), m/e 202, 530 (M).
12. 1 : 2 [2+2]-Photoadduct (see below) was obtained from the photoreaction of duroquinone and 1,4-diethynylbenzene in dichloromethane with 300 nm UV light. Spectral data; IR (KBr), 3057, 2973, 1700, 1665, 1454, 1377, 835 cm^{-1}; UV (MeOH), λ_{max} 290, 280, 257 nm; ^{1}H NMR ($CDCl_3$), δ 7.38 (4H, s, ArH), 6.49 (2 x 1H, s, 2=CH's), 1.97 (2 x 3H, s, 2 Me), 1.93 (2 x 3H, s, 2Me), 1.60 (2 x 3H, s, 2Me), 1.48 ppm (2 x 3H, s, 2Me); ^{13}C NMR ($CDCl_3$), δ 200.4 and 199.8 (C=O's), 134.5 (=CH's), 125.8 (aromatic CH's), 16.93, 16.55, 13.80 and 13.56 (Me's), 152.6, 142.6, 142.5, 132.0, 58.25, 56.08 ppm (6C's); Mass (CI), m/e 455 (M+1).
    Spectral data of the electrocyclic reaction product; IR (KBr), 3043, 2924, 1700, 1644, 1454, 1377, 842 cm^{-1}; UV (MeOH), λ_{max} 336, 294, 254, 240 nm; ^{1}H NMR ($CDCl_3$), δ 7.72 (4H, s, ArH), 7.61 (2H, s, 2=CH'), 2.14 (6H, s, 2Me), 1.71 (6H, s, 2me), 1.41 (6H, s, 2Me), 1.40 ppm (6H, s, 2me); ^{13}C NMR ($CDCl_3$), δ 206.0 and 204.5 (C=O's), 158.9 (=CH's), 127.3 (aromatic CH's), 16.90, 16.29, 12.91 and 8.34 ppm (Me's); Mass (CI), m/e 455 (M+1).

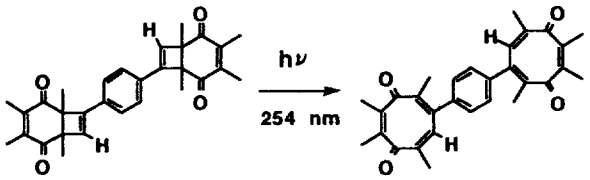

Novel Migration of Aryl Group in 3-Trifluoromethylpyrazolyl Aryl Ether

Kyung-Ho Park, Sung Yun Cho, Sung Soo Kim, Eul Kgun Yum, Chan-Mo Yu†, and Ki-Jun Hwang*

Korea Research Institute of Chemical Technology, P.O. Box 107, Yusung, Taejon 305-606, Korea
†*Department of Chemistry, Sung Kyun Kwan University, Suwon 440-746, Korea*

Received June 13, 1995

3-Trifluoromethylpyrazolyl aryl ethers **2** have been reported to exhibit a potent herbicidal activity[1] and also used as intermediates for the synthesis of insecticides.[2] In the synthesis of their analogues, the aryl group was usually introduced by the reaction of compound **1** with an appropriate aryl halide under basic conditions (Scheme 1).

Surprisingly, in case of R=H, we found that the above reactions initially gave the *O*-arylated pyrazole compound **2** as an intermediate and eventually resulted in the aryl group migrated pyrazole compound **3** with a concomitant formation of regioisomer **4** as a minor product. The progress of reaction can be simply checked by T.L.C. The regioisomers of the reaction products can be assigned by comparing the physical properties and spectral data of the isomers with the ones of the authentic samples, which were synthesized by other methods,[3-8] such as using aryl hydrazine derivatives shown in Scheme 1. The general solubilities[3,5] of the two isomers were reported. So the separation of the two regioisomers was facile since the 5-hydroxy isomer **3** was soluble in aqueous $NaHCO_3$ solution while the 3-hydroxy isomer **4** was not.

Of the several intramolecular rearrangement reaction of aryl group from oxygen to nitrogen atoms, the Chapman Rearrangement,[9] which is the thermal reaction of aryl imidates to *N,N*-diaryl amides, is typical. Just like the Chapman Rearrangement, the strong electron-withdrawing groups of the aryl ring in the above reactions facilitate its migration from oxygen to nitrogen atoms (Table 1). Contrary to the aryl group, no alkyl group migration was observed at all.

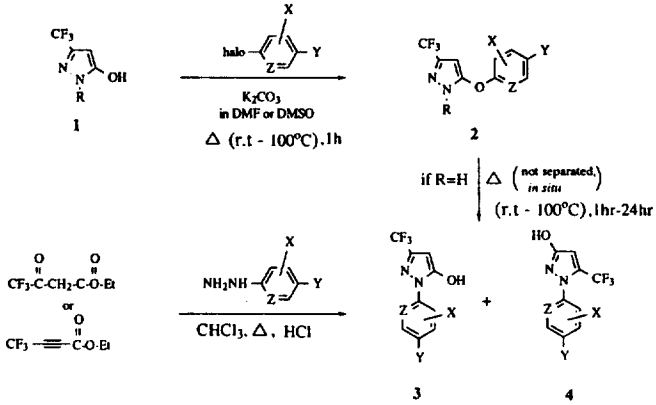

Scheme 1.

Table 1. Aryl-migrated products **3** and **4** in 3-Trifluoromethylpyrazolyl Aryl Ether System **2**

No.	1-halo	X	4-Y	Z	**3** (Yield; mp; MS (EI, m/e); ^{1}H NMR[a])	**4** (Yield; mp; MS (EI, m/e); ^{1}H NMR[a])
1	Cl	H	NO_2	N	77%; 138-140 ℃; 274 (M^+); ($CDCl_3$+Acetone d_6) δ 5.93 (s, 1H), 8.21 (d, J=9.82, 1H), 8.73-8.95 (m, 1H), 9.33 (m, 1H).	not obtained.
2	Cl	2-Cl	NO_2	C	50%; 232-233 ℃; 308 (M^+); ($CDCl_3$) δ 5.92 (s, 1H), 7.85-7.98 (d, J=8.5, 1H), 8.33-8.55 (m, 2H).	17%; 160-162 ℃; 308 (M^+); ($CDCl_3$) δ 6.29 (s, 1H), 7.70-7.81 (d, J=8.5, 1H), 8.25-8.59 (m, 2H), 10.5 (s, broad, 1H).
3	Cl	2,6-Cl_2	NO_2	C	40%; 219-220 ℃; 342 (M^+); ($CDCl_3$+Acetone d_6) δ 5.93 (s, 1H), 8.36 (s, 2H), 10.55 (s, broad, 1H).	10%; 210 ℃; 342 (M^+); ($CDCl_3$+Acetone d_6) δ 6.34 (s, 1H), 8.40 (s, 2H), 9.71 (s, broad, 1H).
4	Br	H	H	N-O^-	40%; 119-120 ℃; 245 (M^+); ($CDCl_3$) δ 5.85 (s, 1H), 7.35-8.52 (m, 4H).	20%; 166-168 ℃ (decomp); 245 (M^+); ($CDCl_3$+d_4-methanol) δ 6.46 (s, 1H), 7.19-7.85 (m, 3H), 8.30-8.51 (m, 1H).
5	Cl	H	CF_3	N	16%; 66-68 ℃; 297 (M^+); ($CDCl_3$) δ 5.91 (s, 1H), 8.11-8.28 (m, 2H), 8.61-8.72 (m, 1H).	4%; 39-40 ℃; 297 (M^+); ($CDCl_3$+DMSO-d_6) δ 5.45 (s, 1H), 8.11-8.22 (m, 2H), 8.89-9.06 (m, 1H).
6	Cl	H	NO_2	C	16%; 159-162 ℃; 273 (M^+); ($CDCl_3$) δ 5.91 (s, 1H), 8.02-8.42 (m, 4H).	not obtained.
7	F	2-F	C≡N	C	16%; 211-212 ℃; 271 (M^+); ($CDCl_3$+Acetone d_6) δ 5.93 (s, 1H), 7.55-7.83 (m, 3H), 9.12 (s, 1H).	not obtained.

[a]Spectra were recorded on either Varian Gemini 200 or JEOL JNM-PMX 60 instrument with TMS as reference.

It is interesting that the intermediate *O*-arylated pyrazole compound **2**, which was isolated from the reaction mixture, did not afford the rearrangement product on heating in organic solvent without base. The addition of base, K_2CO_3, to the solution containing the isolated compound **2** also gave no rearrangement product. So, instead of K_2CO_3, we added the base $KHCO_3$ which might be simultaneously formed at the formation of intermediate **2** in the Scheme 1 reaction conditions, and it gave the migrated product. Therefore whether the migration could occur or not may depend on the base solubility in the reaction mixture.

In conclusion, it was observed that when R in the 3-trifluoromethylpyrazolyl aryl ether **2** was H, the novel migration of aryl group from oxygen to nitrogen atom took place in the presence of base. The mechanism of this reaction is currently under study.

Typical procedure

Synthesis of intermediate 2 (R=H, Z=C, X=2-Cl, Y=4-NO_2). A solution of the 5-hydroxy-3-trifluoromethylpyrazole[10] **1** (R=H, 1 g, 6.57 mmol), 3,4-dichloro-nitrobenzene (1.26 g, 6.57 mmol) and potassium carbonate (1.36 g, 9.86 mmol) in DMF (10 mL) was stirred at 100 ℃ for 4 hours. After cooling to room temperature, ethyl acetate (80 mL) was added to the reaction mixture and the reaction mixture was washed with water (20 mL×3), and dried ($MgSO_4$). The solvent was evaporated to leave the pyrazolylaryl ether, which was purified by chromatography on silica gel (ethyl acetate-hexane 1 : 9) to give 1.5 g (Yield: 74%) of **2**: mp 94-95 ℃; MS (EI) m/e 308 (M^+); ^{1}H NMR ($CDCl_3$) δ 6.29 (s, 1H), 7.22-7.43 (m, 1H), 8.12-8.55 (m, 2H).

Synthesis of aryl-migrated products 3 and 4 (Table 1, No. 2; Z=C, X=2-Cl, Y=4-NO_2) by *in-situ* method. The same scale reaction as described above was carried out at 100 ℃ for 4 hours. At this stage of reaction the formation of intermediate **2** (R=H, Z=C, X=2-Cl, Y=4-NO_2) was detected by T.L.C. (silica gel, ethyl acetate-hexane 1 : 3). Further reaction at 100 ℃ for 10 hours allowed totally to consume intermediate **2** and to produce **3** and **4** which were detected on T.L.C. (silica gel, ethyl acetate-hexane 1 : 3). Ethyl acetate (50 mL) was added to the reaction mixture at room temperature, and the solution was washed with water (20 mL×2). The organic layer was dried ($MgSO_4$), and evaporated to give one of the isomers **4**, which was further purified by chromatography on silica gel (ethyl acetate-hexane 1 : 9) to give 0.34 g of **4**. The aqueous layer was acidified by 5% HCl (20 mL) and extracted with ethyl acetate (50 mL). The organic layer was dried ($MgSO_4$), evaporated, and purified by chromatography on silica gel (ethyl acetate-hexane 1 : 3) to give 1.01 g of the other isomer **3**. Yield, mp, MS, and ^{1}H NMR for **3** and **4** are given in Table 1.

References

1. Sherman, T. D.; Duke, M. V.; Clark, R. D.; Sanders, E. F.; Matsumoto, H.; Duke, S. O. *Pest. Biochem. Physiol.* **1991**, *40*, 236.

2. Hwang, K. J.; Park, K. H. *U.S. Pat.* 5,389,667.
3. Lee, L. F.; Schleppnik, F. M.; Schneider, R. W.; Campbell, J. W. *J. Heterocyclic Chem.* **1990**, *27*, 243.
4. Moedritzer, K.; Rogers, M. D. *U.S. Pat.* 4,964,895.
5. Lee, L. F.; Moedritzer, K.; Rogers, M. D. *U.S. Pat.* 4,855, 442.
6. Gaede, B. J.; Torrence, L. L. *U.S. Pat.* 4,984,902.
7. Hamper, B. C. *J. Fluorine Chem.* **1990**, *49*, 23.
8. Hamper, B. C.; Kurtzweil, M. L.; Beck, J. P. *J. Org. Chem.* **1992**, *57*, 5680.
9. (a) Chapman, A. W. *J. Chem. Soc.* **1925**, *127*, 1992. (b) March, J. *Advanced Organic Chemistry*, 4th Ed.; John Wiley & Sons: New York, 1992; p 1155.
10. DeStevens, G.; Halamandaris, A.; Wenk, P.; Dorfman, L. *J. Am. Chem. Soc.* **1959**, *81*, 6292.

Dynamics of OH Photodissociation above the Threshold to O(^1D): A Quantum Mechanical Analysis

Sungyul Lee

Department of Chemistry, College of Natural Sciences, Kyunghee University, Kyungki-do 449-701, Korea

Received June 13, 1995

Diatomic photodissociation processes are very important in molecular reaction dynamics for several reasons. *Ab initio* results on the potential energy curves, transition dipole moments and nonadiabatic interactions of many diatomic molecules are avalable for detailed dynamic calculations. The theory of photodissociation[1] is well developed so that direct comparison between theoretical calculations and experiments are now possible. Developments of powerful experimental methods such as multiphoton technique has made it possible to probe the dynamic processes of molecules at wide ranges of excitation energy.

In a series of papers,[2~8] we have shown that the exact treatments of the photodissociation processes are very useful for elucidating many interesting dynamic behaviors of molecules. It has been demonstrated that nonadiabatic interactions both in the Franck-Condon region and in asymptotic region can significantly affect such important dynamic observables as the shape of the resonances,[2,4~6] product branching ratios[4~6] and angular distributions.[7,8] The magnitude of these influences has been found to be large at energies below the threshold to O(^1D) in the photodissociation of OH molecule. Crossings between the bound $A^2\Sigma^+$ and the repulsive $^4\Sigma^-$, $^2\Sigma^-$ and $^4\Pi$ states result in well-known predissociation in this energy regime, and quantum interference between the indirect dissociation pathway *via* $A^2\Sigma^+$ state and the direct dissociation pathway through $^2\Sigma^-$ state has been predicted[2,4~6] to give rise to asymmetric resonances in the photodissociation cross sections. It has also been shown that

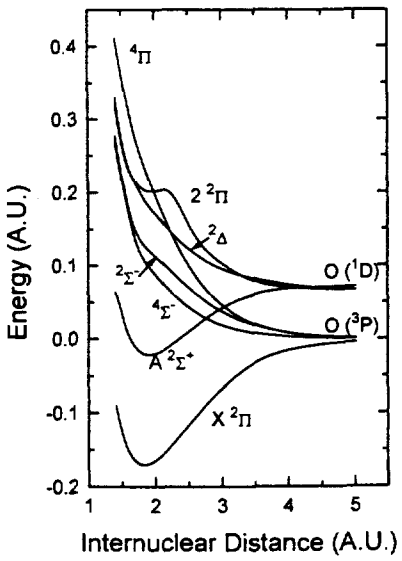

Figure 1. Potential curves of OH.

the branching ratios of O(^3P_j, $j=0$, 1, 2) exhibit rapid variations near these asymmetric resonances.[4~6] Implications of this latter finding have been discussed in the spirit of coherent control of dynamic processes.

Above the dissociation threshold to O(^1D), all of the potential curves (including $A^2\Sigma^+$) are dissociative (see Figure 1), and the dissociation is direct in this energy regime. It is well known[9] that the direct dissociation processes approach a diabatic limit at high kinetic energies of the photofragments, which are characterized by energy independent product branching ratios and angular distributions. Actually, it is in this high energy regime that particular values of the observables can be correlated with the symmetries of the excited states and dissociation pathways in a simple fashion.[9,10] We demonstrate in this work that dissociations to O(^3P) fragments show signs of diabatic limit behaviors at energies above the threshold to O(^1D). However, dissociation processes to O(^1D) exhibit very different patterns, characterized by highly oscillating fragment anisotropy parameters, as a result of the quantum interference between two direct dissociating pathways.

The theory has been described in detail elsewhere,[6] and we only give a brief summary in this paper. Since the two oxygen atomic term limits, O(^3P) and O(^1D), are involved in OH photodissociation (see Figure 1), we construct two transformation matrices,[6,9] each of which describes the connections between an atomic term and adiabatic Born-Oppenheimer states correlating with it. Two kinds of basis functions are employed in the calculations to evaluate the total Hamiltonian. Hund's case (a) basis function of parity p, $|JM C\Lambda S\Sigma p\rangle$ is employed to evaluate the electronic Hamiltonian, which is diagonal in this basis. J is the total angular momentum, M is its component along the space-fixed axis, S is the total spin, Λ and Σ are the components of J and S along the molecular axis, respectively, and C denotes any other electronic state labels. The asymptotic basis functions $|JMjlC_0j_0j_H\rangle$ are used to evaluate the spin-orbit Hamiltonian and the rotational part $l(l+1)/2\mu r^2$, since they are diagonal in these basis functions. Here j_0 (j_H) are the total electronic